American Journal of Materials Science and Engineering, 2015, Vol. 3, No. 1, 15-20
Available online at http://pubs.sciepub.com/ajmse/3/1/4

DOI:10.12691/ajmse-3-1-4

The Effect of Iridium Addition to Platinum on the Alcohol Electrooxidation Activity

Ozlem Sahin[1], Hilal Kivrak[2,*], Mustafa Karaman[1], Dilan Atbas[2]

[1]Chemical Engineering Department, Selcuk University, Konya, Turkey
[2]Chemical Engineering Department, Yüzüncü Yıl University, Van Turkey
*Corresponding author: hilalkivrak@gmail.com, hilalkivrak@yyu.edu.tr

Received May 26, 2015; Revised July 24, 2015; Accepted July 27, 2015

Abstract Pt-Ir@C and Pt@C catalysts were prepared by ethylene glycol method and tested for methanol and ethanol in H_2SO_4 electrolyte. The electrocatalytic activity of these electrocatalysts was investigated using cyclic voltammograms (CVs), linear sweep voltammograms (LSVs), chronoamperometry (CA) and electrochemical impedance spectroscopy (EIS). Their CVs show that $Pt_{40}Ir_{60}$@C catalyst present significantly high current of methanol and ethanol oxidation compared to the other catalysts. Moreover, chronoamperometric measurements showed that the steady-state current of $Pt_{40}Ir_{60}$ catalyst was also higher than other electro-catalysts. EIS analysis shows that the impedances on both the imaginary and real axes are much lower than those of the other catalysts. As a result, electrocatalytic activity measurements indicated that the $Pt_{40}Ir_{60}$ catalyst was the most active electrode for methanol and ethanol oxidation.

Keywords: *Pt-Ir, alcohol, electrooxidation, fuel cells, CV, CA, impedance*

Cite This Article: Ozlem Sahin, Hilal Kivrak, Mustafa Karaman, and Dilan Atbas, "The Effect of Iridium Addition to Platinum on the Alcohol Electrooxidation Activity." *American Journal of Materials Science and Engineering*, vol. 3, no. 1 (2015): 15-20. doi: 10.12691/ajmse-3-1-4.

1. Introduction

Direct alcohol fuel cells (DAFCs) based on liquid fuels have attracted considerable interest due to the depletion of fossil fuels and the increase in environmental pollution. Direct methanol fuel cells (DMFCs) and direct ethanol fuel cells (DEFCs) are excellent power sources among different types of fuel cells. The main advantage of methanol and ethanol is that they are liquid. Thus, the storage problems when hydrogen is used are solved. Additionally, the power density of the alcohols in terms of energy by volume of fuel is much higher at standard conditions. When comparing methanol and ethanol fuels, the attention is focused on the use of methanol because of its better reaction kinetics. Hence, DMFCs give better performance than DEFCs. However, ethanol has received considerable interest due to several reasons as follows: (i) its low toxicity, (ii) easy production in large amounts as renewable biofuel from the fermentation of biomass, (iii) higher energy density, and (iv) abundant availability [1-5].

Pt is known active and stable metal for alcohol oxidation especially in acidic medium. Nevertheless, Pt is readily poisoned by CO-like intermediates of alcohol electrooxidation. The effective approach is to use Pt alloys to enhance the electrocatalyst activity [6,7,8,9]. Among these Pt alloys, the recent researches have focused on the development of Pt-Sn and Pt-Ru alcohol electrocatalysts due to the effective for CO and alcohol oxidation [10-15]. Tsiakaras et al. conducted a study on Pt-Sn/C catalysts at different atomic ratios by using a single DEFC at 60°C and 90°C. It was reported that Pt-Sn (3:2)/C catalyst revealed the highest MPD at 60°C. On the contrary, the OCV and MPD of Pt-Sn (1:1)/C was smaller than that of Pt-Sn (3:2)/C catalyst, attributed to the fact that platinum active sites of catalysts with a high Sn content could be partly blocked by surface tin or its oxides [16]. The decoration of carbon supported Pt with Sn, the decoration of carbon supported Sn with Pt, and the co-deposition of Pt and Sn on carbon were the different preparation orders to investigate the effect of preparation orders on the formation of oxide phases and on the electrochemical activity [17]. As a result, Sn decorated Pt showed the best performance for ethanol electro-oxidation reaction and XPS data showed that Sn existed as Sn oxides in the Pt-Sn catalyst. Jiang et al. conducted as study on Pt_3Sn/C catalyst prepared by a modified polyol process and treated in O_2, H_2/Ar, and Ar atmosphere, respectively. In consequence, among these treated catalysts, the as-prepared Pt-Sn/C catalyst gave the higher power density, while Ar-treated Pt-Sn/C showed the lower cell performance. This is due to the fact that more zero valence of Sn appeared in Pt-Sn/C-Ar catalyst, while more multi-valence Sn existed in the other catalysts [18,19]. Other binary catalysts Pt-Pd [16], Pt-W [16], Pt-Re [20], Pt-Rh [21-26], Pt-Pb [27,28], Pt_3Tex [29], Pt-Sb [30], Pt-CeO_2 [31,32,33,34], Pt-ZrO_2 [31,35], Pt-MgO [36], Pt-TiO_2 [37,38,39,40,41], Pt-SiO_2 [42] were investigated for ethanol electro-oxidation reaction. Generally these catalysts presented lower activity than that of Pt and lower than that of Pt-Ru.

Harish and coworkers [10] employed a polyol process activated by microwave irradiation to prepare efficient Pt/C, Ru/C and Pt-Ru/C electrocatalysts. Pt-Ru/C catalyst displayed a high activity towards CO and methanol electrooxidation activity (MOR). Furthermore, the lowest onset potentials and lowest surface poisoning of MOR for Pt-Ru catalysts than those obtained on Pt/C catalysts were observed.

Other binary or ternary/quaternary Pt alloys catalysts have been paid less attention to enhance the performance of Pt catalysts. Ir is unique among them, because Ir has a relatively high oxidation potential of because Ir can react with water to produce Ir–OH species, which will combine with Pt– CO species to remove surface-adsorbed CO at the potential lower than pure Pt. [43].

Herein, Pt-Ir@C and Pt@C electrocatalysts were prepared by polyol method at different weight percentages of Ir. These catalysts prepared at varying Pt: Ir ratios were examined as DAFC catalysts to investigate the effect of Ir ratio.

2. Materials and Methods

Carbon black (Vulcan XC72R) was purchased from Cabot Corp. CH_3OH, CH_3CH_2OH, H_2SO_4, KOH, $H_2PtCl_6.6H_2O$, and $IrCl_3.xH_2O$ were purchased from Merck and Aldrich. All chemicals were of analytical grade and were used as received.

Pt@C and Pt-Ir@C catalysts were prepared by ethylene glycol reduction method [15]. For Pt/C catalyst, $H_2PtCl_6.6H_2O$ and for Pt-Ir catalysts $H_2PtCl_6.6H_2O$ and $IrCl_3.xH_2O$ were dissolved in 200 mL ethylene glycol solution per gram carbon support. The pH of the solution was fixed at 10 by the addition of KOH solution and carbon support was dispersed in this solution. Consequently, the temperature was increased to 130°C and kept constant at this temperature for 2 h. After refluxing at 130°C for 2 h, the slurry suspension was rapidly cooled down in cold water, filtered, and dried. Pt-Ir@C catalysts were prepared at varying 80:20, 40:60, and 20:80 Pt: Ir atomic ratios. Nominal Pt loadings of all catalysts are 10%.

XRD patterns were measured on a Bruker D 8 Advance X-Ray diffractometer using Cu Kα-ray radiation (k = 1.5405 A°) operating at 30 kV and 15 mA. XRD patterns were recorded between 2h = 10.0–100.0° with 0.05° intervals, 1° data collection velocity in 1 min.

Surface characterization of catalysts for the oxidation states of the surface species X-ray Photoelectron Spectroscopy (XPS) was performed. The X-ray photoelectron spectra was obtained using Mg-Kα (hv = 1253.6 eV) unmonochromatized radiation with SPECS spectrometer. The charging effects were corrected by using the C 1s peak, as reference for all samples at a binding energy (BE) of 284.8 eV.

Electrochemical measurements were carried out in a conventional three-electrode cell with Pt wire as a counter electrode and Ag/AgCl as a reference electrode with a CHI 660E potentiostat. The working electrode was a glassy carbon disk with a diameter of 3.0 mm held in a Teflon cylinder. Cyclic voltammograms (CVs) were recorded between -0.25 V and 1 V with a scan rate of 100 mV s^{-1} in 0.5 M H_2SO_4 solution on these catalysts. Furthermore, CV and CA techniques were employed to examine the MOR and EOR activities of Pt@C and Pt-Ir@C catalysts. In all experiments, the electrolyte was previously saturated by nitrogen. Before each experiment, the electrode surface was activated in 0.5 M H_2SO_4. For MOR, CVs were recorded between -0.25 V and 1.0 V with a scan rate of 100 mV s^{-1} in 0.5 M H_2SO_4 + 1.0 M CH_3OH at 25°C. For EOR, CVs were recorded between -0.25 V and 1.0 V with a scan rate of 100 mV s^{-1} in 0.5 M H_2SO_4 + 1 M C_2H_5OH at 25°C. For MOR, chronoamperomograms (CAs) were recorded in 0.5 M H_2SO_4 + 1 M CH_3OH solution on Pt-Ir@C catalysts. Moreover, CA was performed in 0.5 M H_2SO_4 + 1 M C_2H_5OH solution at 0.6 V for 200 s with 1000 s pulse width and 2 s quiet times.

Electrochemical impedance spectroscopy (EIS) as a dynamic method was used to examine the electrochemical behavior of Pt@C and Pt-Ir@C catalysts. EIS measurements were recorded between 30 kHz and 0.01 Hz at amplitude of 10 mV at the desired electrode potential.

3. Results and Discussion

XRD patterns of Pt-Ir@C catalysts were illustrated in Figure 1, which reveal the structural information for the bulk of catalyst nanoclusters together with the carbon support. The diffraction peak at around 25° was attributed to the (002) plane of the hexagonal structure of Vulcan XC-72R carbon. The diffraction peaks at around 39°, 46°, 68° and 81° are due to diffraction of Pt (111), (200), (220) and (311) planes, respectively. For these catalysts, Ir peaks were observed when 40:60 Pt:Ir ratio was reached. It is clear that crystallinity of Pt catalyst decrease by the addition of the Ir due to ensemble size effect [43].

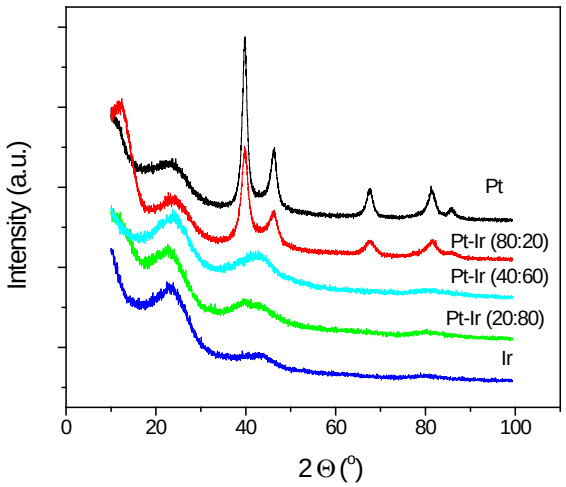

Figure 1. XRD patterns of Pt@C and Pt-Ir@C catalysts

XPS analyses are performed to investigate the chemical nature of these catalysts. High resolution Pt 4f and Ir 4d XPS scans were obtained to investigate the chemical nature of alloys having different compositions. Figure 2 a and Figure 2b shows Pt and Ir XPS spectra together with the spectrum deconvolutions. Curve fitting of the Pt 4f and Ir 4d spectra gives three different types of Pt moieties and two different types of Ir moieties, respectively. Binding energy values for each moiety and the corresponding peak area ratios are summarized in Table 1.

According to the results, the films consist of Pt, Ir, PtO, IrO_2 and $Pt(OH)_2$ states. A rough estimate of atomic mole percentage of each species using relative intensities of XPS peaks reveal that Pt in its elemental state contains around 26 mol% PtO-$Pt(OH)_2$ species. The change of Ir composition in the alloy had little effect on relative amounts of Ir and IrO_2. In the case of Pt/Ir alloys, the oxygen related species tend to composition of Ir in the alloy increases, the amount of such oxygen related species decrease the alloys contain.

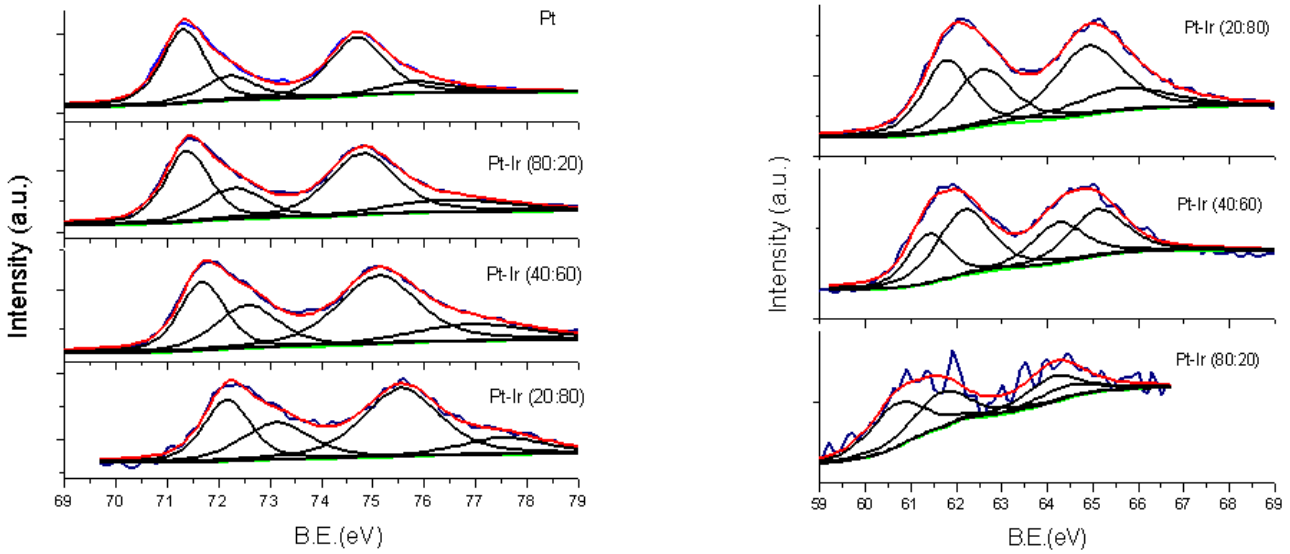

Figure 2. a. Pt 4f XPS spectra of Pt@C and Pt-Ir@C catalysts, **b.** Ir 4d spectra of Pt@C and Pt-Ir@C catalysts

Table 1. Pt 4f and Ir 4 d binding energies of Pt and Pt-Ir electrocatalysts

Catalyst	Species	Binding energy (eV)	Possible Chemical State	Relative Intensity
Pt/C	Pt 4f	71.319	Pt^0	36.4
		72.234	PtO	16.9
		74.69	Pt^0	37.1
		75.837	$Pt(OH)_2$	9,6
Pt-Ir (80:20)/C	Pt 4f	71.396	Pt^0	38,5
		72.304	PtO	29,5
		74.8	Pt^0	14,1
		76.489	$Pt(OH)_2$	17,9
	Ir 4d	60.701	Ir^0	34,2
		61.665	IrO_2	30,7
		64.114	Ir^0	23,5
		64.362	IrO_2	11,5
Pt-Ir (40:60)/C	Pt 4f	71.69	Pt^0	40,8
		72.575	PtO	23.3
		73.897	Pt^0	15.4
		75.732	$Pt(OH)_2$	20.5
	Ir 4d	61.389	Ir^0	25.4
		62.177	IrO_2	34.2
		64.308	Ir^0	20.6
		65.11	IrO_2	19.8
Pt-Ir (20:80)/C	Pt 4f	72.168	Pt^0	23.4
		73.132	PtO	21.5
		75.55	Pt^0	42.8
		77.56	$Pt(OH)_2$	12.3
	Ir 4d	61.793	Ir^0	34.6
		62.589	IrO_2	25.7
		64.919	Ir^0	16.3
		65.654	IrO_2	24.1

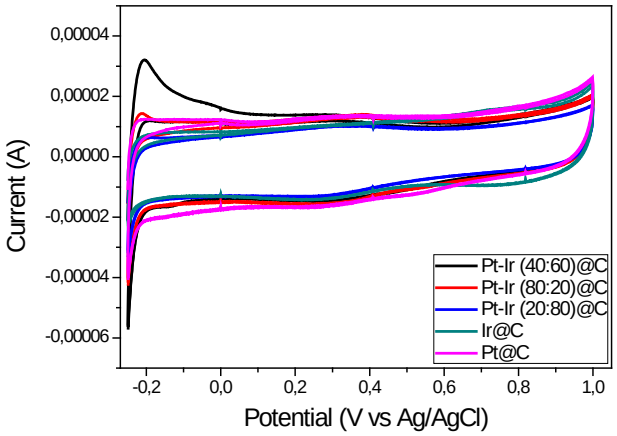

Figure 3. CVs of Pt@C and Pt-Ir@C catalysts in 0.5 M H_2SO_4 at 100 mVs^{-1}

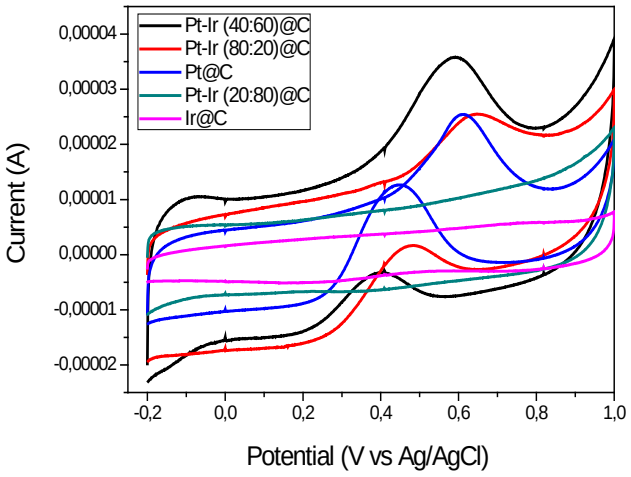

Figure 4. CVs of Pt@C and Pt-Ir@C catalysts in in 0.5 M H_2SO_4 + 1.0 M CH_3OH at 100 mV s^{-1}

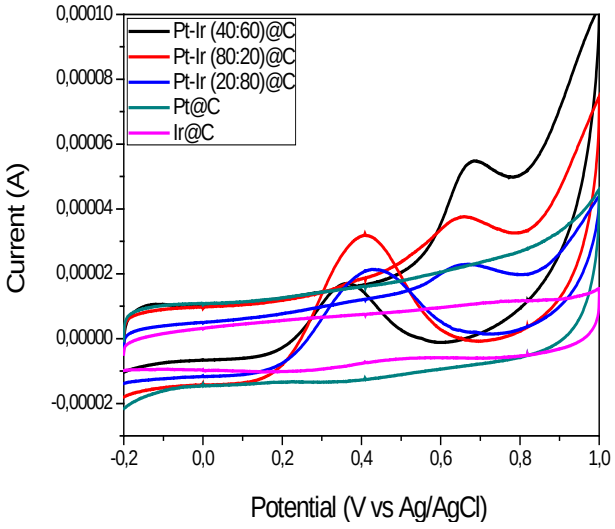

Figure 5. CVs of Pt@C and Pt-Ir@C catalysts in in 0.5 M H_2SO_4 + 1.0 M C_2H_5OH at 100 mV s^{-1}

The cyclic voltammograms (CVs) taken in 0.5 M H_2SO_4 for the Pt@C and Pt-Ir@C catalysts shown in Figure 3. The Pt-Ir electrocatalysts do not have a very defined hydrogen oxidation region (-0.2–0.0 V), as observed for pure platinum, and the currents in the double layer region (0.0–0.4 V) are larger, which are characteristic of bimetallic catalysts. The CVs taken for MOR and EOR measurements on Pt@C and Pt-Ir@C catalysts at a scan rate of 100 mVs^{-1} were given in Figure 4 and Figure 5, respectively.

Obviously, the peaks on the Pt_{40}-Ir_{60}@C electrodes are much stronger than that on the Pt@C and other Pt-Ir@C catalysts, which suggests the Pt_{40}-Ir_{60}@C catalyst has better catalytic activity. Cyclic voltammograms obtained for MOR and EOR on Pt-Ir@C catalysts, have one anodic peak in the forward scan and one oxidation peak in the backward scan showing similar voltammetric behavior as the Pt catalyst. The presence of Ir in the structure of platinum promotes the electrocatalytic activity of platinum towards MOR and EOR. However, the oxidation currents increase reaches the optimum value up to 40:60 Pt:Ir ratio. The role of iridium addition on MOR and EOR can be attributed to the oxidation of Ir at relatively low positive potentials, assisting the redox process of Pt^0/Pt^{2+} or Pt^{2+}/Pt^{4+} [10-15]. These redox processes may play an important part on MOR. The reverse anodic peak observed in the MOR can be attributed to the oxidative removal of incompletely oxidized carbonaceous species strongly adsorbed on the Pt sites, formed in the forward scan. The maximum current ratios of forward to reverse peaks obtained from the CV curves for MOR and EOR were given in Table 2 and Table 3, respectively. One can see that Pt_{40}-Ir_{60}@C catalyst have high I_f/I_b ratios that are closely related to the less accumulation of reaction intermediates during the forward scan and shows low reverse anodic peak current during reverse scan for MOR and EOR. I_f/I_b ratios becomes greater with the increase in the Ir ratio for MOR and EOR, attributed to the presence of Ir in Pt-Ir alloy enhances the catalytic activity and improves the CO conversion to CO_2. Furthermore, I_f /I_b ratio for MOR was higher than the EOR for catalysts having the Pt: Ir same ratio. Pt_{40}-Ir_{60}@C catalyst showed the best performance which could be attributed to the presence of more iridium oxide species on the nanoparticles surface. Hence, the ratio of forward peak to the reverse peak describes the catalyst tolerance to carbonaceous species accumulation formed on the catalyst during the forward potential scan. The high I_f /I_b ratio indicated that the addition of Ir to the Pt enhances the CO conversion to CO_2, and less accumulation of carbonaceous species on the catalyst. On the other hand, the high If/I_b ratio indicates excellent MOR during the reverse anodic scan and less accumulation of residues on the catalyst [6,7,8,9].

Table 2. Comparison of electrocatalytic activity of MOR on Pt@C and Pt-Ir@C catalysts

Catalyst	Forward sweep		Reverse sweep		I_f/I_b Ratio
	I_F x10^{-5}(A)	E (V)	I_R x10^{-5}(A)	E (V)	
$Pt_{40}Ir_{60}$@C	2.5	0.57	1.0	0.4	2.5
$Pt_{80}Ir_{20}$@C	2.0	0.60	2.5	0.45	0.8
$Pt_{20}Ir_{80}$@C	-	-	-	-	-
Pt@C	1.5	0.59	2.0	0.43	0.75
Ir@C	-	-	-	-	-

Table 3. Comparison of electrocatalytic activity of EOR on Pt@C and Pt-Ir@C catalysts

catalyst	Forward sweep		Reverse sweep		I_f/I_b Ratio
	I_F x10^{-5}(A)	E (V)	I_R x10^{-5}(A)	E (V)	
$Pt_{40}Ir_{60}$@C	4.0	0.62	2.5	0.41	0.66
$Pt_{80}Ir_{20}$@C	2.5	0.64	5.0	0.46	0.5
$Pt_{20}Ir_{80}$@C	-	-	-	-	-
Pt@C	1.0	0.67	3.0	0.51	0.33
Ir@C	-	-	-	-	-

The catalytic activities and stability of Pt@C and Pt-Ir@C catalysts have also been investigated by chronoamperometry. Figure 6 and Figure 7 show the current vs time curves of catalysts measured at 0.6 V for MOR and EOR, respectively. The shape of the CA curves obtained in methanol solution is similar to those obtained in ethanol solution. There is a continuous current drop with time for MOR and EOR, which is rapid at the beginning and then followed by a relatively slow decay. The higher initial current means a greater number of active sites available for oxidation. It is demonstrated that the higher catalytic activity and better stability are achieved on the Pt_{40}-Ir_{60}@C catalyst for MOR and EOR.

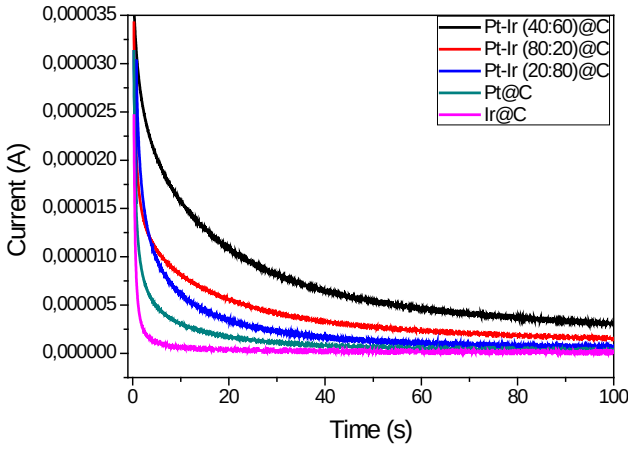

Figure 6. CAs of Pt@C and Pt-Ir@C catalysts in in 0.5 M H_2SO_4 + 1.0 M CH_3OH at 0.6 V

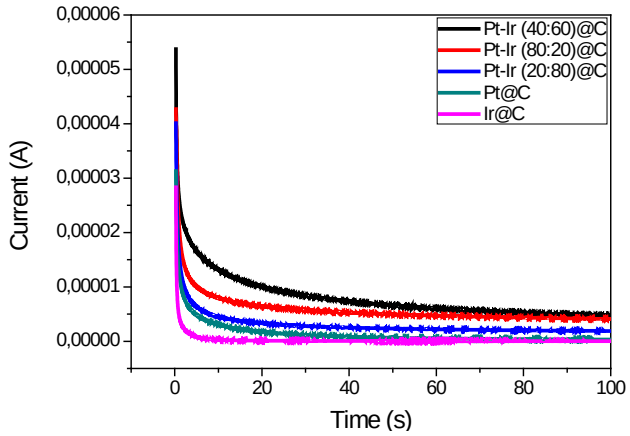

Figure 7. CAs of Pt@C and Pt-Ir@C catalysts in 0.5 M H_2SO_4 + 1.0 M C_2H_5OH at 0.6V

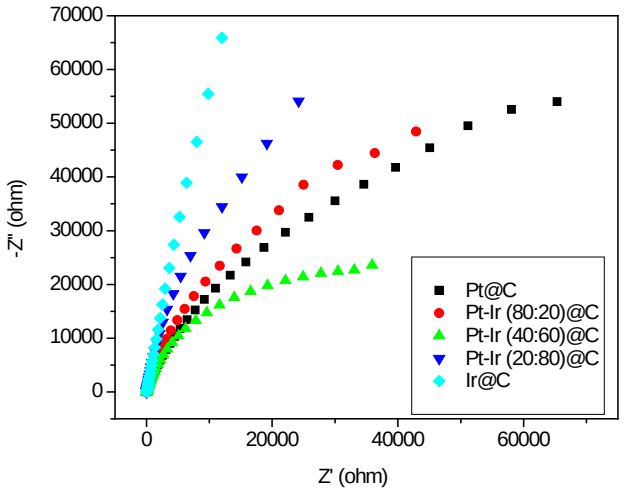

Figure 8. Nyquist plots of Pt@C and Pt-Ir@C catalysts in 0.5 M H_2SO_4 + 1.0 M CH_3OH

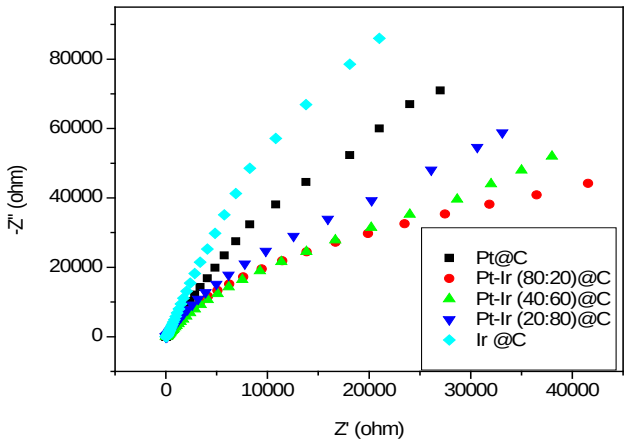

Figure 9. Nyquist plots of Pt@C and Pt-Ir@C catalysts in 0.5 M H_2SO_4 + 1.0 M C_2H_5OH

Electrochemical impedance spectroscopy (EIS) is a powerful technique to control the activity of the catalyst to analyze the electrochemical processes occurring at the electrode interface. Figure 8 and Figure 9 presents a typical electrochemical impedance spectrum in the form of a Nyquist plot of Pt@C and Pt-Ir@C catalysts for MOR and EOR respectively. At initial lower potentials, a large arc appears and the diameter of this arc decreases with potential. The semicircle diameter equals to the electron-transfer resistance, which is affected obviously by the surface modification of the electrode. The initial slow kinetics is caused by CO_{ad} from alcohol dehydrogenation that blocks further adsorption and dehydrogenation of alcohol. As shown in Figure 7, the electron-transfer resistance of the Pt_{40}-Ir_{60}@C catalyst is less than that of the Pt@C and other Pt-Ir@C catalysts, revealing that iridium oxide species formed can enhance the conductivity of the electrode owing to its faster interfacial charge carrier transfer as a result of higher oxide formation. Usually, conductivity and surface activity are two important factors for a good analytical electrode. Therefore, the Pt_{40}-Ir_{60}@C catalyst possesses excellent performance in MOR and EOR [15].

4. Conclusions

As a conclusion, the study of the preparation, characterization and employment of Pt@C and Pt-Ir@C catalysts has led to the following conclusions and insights:

- Pt-Ir nanoparticles could be easily prepared from the co-reduction of corresponding platinum and Ir salts by polyol method.
- Pt_{40}-Ir_{60}@C catalyst is highly efficient catalyst for MOR activity compared to Pt@C and other Pt-Ir@C catalysts.
- The Ir addition to Pt increases the activity of alcohol electrooxidation until and 40: 60 optimum ratio was reached.
- One can note that iridium oxide species increased by the addition of Ir at 40: 60 optimum ratio. This iridium oxide species can enhance the conductivity of the electrode owing to its faster interfacial charge carrier transfer as a result of higher oxide formation. Therefore, the Pt_{40}-Ir_{60}@C catalyst possesses excellent performance in MOR and EOR.

Acknowledgement

Authors would like to thank The Administrative Units of the scientific research projects of Selcuk University for the financial support (project no: S.U. 13401011).

References

[1] Kashyout AB, Nassr AAA, Giorgi L, Maiyalagan T, Youssef BAB. Electrooxidation of Methanol on Carbon Supported Pt-Ru Nanocatalysts Prepared by Ethanol Reduction Method. *International Journal of Electrochemical Science*.6(2).379-393. Feb 2011

[2] Perez J, Paganin VA, Antolini E. Particle size effect for ethanol electro-oxidation on Pt/C catalysts in half-cell and in a single direct ethanol fuel cell. *Journal of Electroanalytical Chemistry*. 654(1-2).108-115. May 2011.

[3] Cimenti M, Hill JM. Direct utilization of ethanol on ceria-based anodes for solid oxide fuel cells. Asia-Pacific Journal of Chemical Engineering. 4(1).45-54. Jan-Feb 2009.

[4] Fujiwara N, Siroma Z, Yamazaki SI, Ioroi T, Senoh H, Yasuda K. Direct ethanol fuel cells using an anion exchange membrane. *Journal of Power Sources*. 185(2).621-626. Dec 2008.

[5] Antolini E. Catalysts for direct ethanol fuel cells. *Journal of Power Sources*. 170(1).1-12. Jun 2007.

[6] Neto AO, Farias LA, Dias RR, Brandalise M, Linardi M, Spinace EV. Enhanced electro-oxidation of ethanol using PtSn/CeO2-C electrocatalyst prepared by an alcohol-reduction process. *Electrochemistry Communications*. 10(9).1315-1317. Sep 2008.

[7] Li HQ, Sun GQ, Cao L, Jiang LH, Xin Q. Comparison of different promotion effect of PtRu/C and PtSn/C electrocatalysts for ethanol electro-oxidation. *Electrochimica Acta*.52(24).6622-6629. Aug 2007.

[8] Simoes FC, dos Anjos DM, Vigier F, et al. Electroactivity of tin modified platinum electrodes for ethanol electrooxidation. *Journal of Power Sources*. 167(1).1-10. May 2007.

[9] Jiang LH, Zang HX, Sun GQ, Xin Q. Influence of preparation method on performance of PtSn/C anode electrocatalyst for direct ethanol fuel cells. *Chinese Journal of Catalysis*. 27(1).15-19. Jan 2006.

[10] Harish S, Baranton S, Coutanceau C, Joseph J. Microwave assisted polyol method for the preparation of Pt/C, Ru/C and PtRu/C nanoparticles and its application in electrooxidation of methanol. *Journal of Power Sources*. 214.33-39. Sep 15 2012.

[11] Zhang L, Kim J, Chen HM, et al. A novel CO-tolerant PtRu core-shell structured electrocatalyst with Ru rich in core and Pt rich in shell for hydrogen oxidation reaction and its implication in proton exchange membrane fuel cell. *Journal of Power Sources*. 196(22).9117-9123. Nov 2011.

[12] Lee KS, Park HY, Cho YH, Park IS, Yoo SJ, Sung YE. Modified polyol synthesis of PtRu/C for high metal loading and effect of post-treatment. *Journal of Power Sources*. 195(4).1031-1037. Feb 2010.

[13] Carmo M, Roepke T, Scheiba F, et al. The use of a dynamic hydrogen electrode as an electrochemical tool to evaluate plasma activated carbon as electrocatalyst support for direct methanol fuel cell. *Materials Research Bulletin*. 44(1).51-56. Jan 2009.

[14] Li J, Liang Y, Liao Q, Zhu X, Tian X. Comparison of the electrocatalytic performance of PtRu nanoparticles supported on multi-walled carbon nanotubes with different lengths and diameters. *Electrochimica Acta*. 54(4).1277-1285. Jan 2009.

[15] Sahin O, Kivrak H. A comparative study of electrochemical methods on Pt-Ru DMFC anode catalysts. The effect of Ru addition. *International Journal of Hydrogen Energy*. 38(2).901-909. Jan 24 2013.

[16] Tsiakaras PE. PtM/C (M = Sn, Ru, Pd, W) based anode direct ethanol-PEMFCs. Structural characteristics and cell performance. *Journal of Power Sources*. 171(1).107-112. Sep 2007.

[17] Li GC, Pickup PG. Decoration of carbon-supported Pt catalysts with Sn to promote electro-oxidation of ethanol. *Journal of Power Sources*. 173(1).121-129. Nov 2007.

[18] Jiang LH, Zhou ZH, Li WZ, et al. Effects of treatment in different atmosphere on Pt3Sn/C electrocatalysts for ethanol electro-oxidation. *Energy & Fuels*. 18(3).866-871. May-Jun 2004.

[19] Jiang LH, Zhou ZH, Zhou WJ, et al. Synthesis, characterization and performance of PtSn/C electrocatalyst for direct ethanol fuel cell. *Chemical Journal of Chinese Universities-Chinese*. 25(8).1511-1516. Aug 2004.

[20] Vigier F, Coutanceau C, Perrard A, Belgsir EM, Lamy C. Development of anode catalysts for a direct ethanol fuel cell. *Journal of Applied Electrochemistry*. 34(4).439-446. Apr 2004.

[21] Bergamaski K, Gonzalez ER, Nart FC. Ethanol oxidation on carbon supported platinum-rhodium bimetallic catalysts. *Electrochimica Acta*. 53(13).4396-4406. May 2008.

[22] de Souza JPI, Queiroz SL, Bergamaski K, Gonzalez ER, Nart FC. Electro-oxidation of ethanol on Pt, Rh, and PtRh electrodes. A study using DEMS and in-situ FTIR techniques. *Journal of Physical Chemistry B*. 106(38).9825-9830. Sep 2002.

[23] Kowal A, Gojkovic SL, Lee KS, Olszewski P, Sung YE. Synthesis, characterization and electrocatalytic activity for ethanol oxidation of carbon supported Pt, Pt-Rh, Pt-SnO2 and Pt-Rh-SnO2 nanoclusters. *Electrochemistry Communications*. 11(4).724-727. Apr 2009.

[24] Kowal A, Li M, Shao M, et al. Ternary Pt/Rh/SnO2 electrocatalysts for oxidizing ethanol to CO2. *Nature Materials*. 8(4).325-330. Apr 2009.

[25] Lima FHB, Gonzalez ER. Electrocatalysis of ethanol oxidation on Pt monolayers deposited on carbon-supported Ru and Rh nanoparticles. *Applied Catalysis B-Environmental*. 79(4).341-346. Mar 2008.

[26] Lima FHB, Gonzalez ER. Ethanol electro-oxidation on carbon-supported Pt-Ru, Pt-Rh and Pt-Ru-Rh nanoparticles. *Electrochimica Acta*. 53(6).2963-2971. Feb 2008.

[27] Li GC, Pickup PG. The promoting effect of Pb on carbon supported Pt and Pt/Ru catalysts for electro-oxidation of ethanol. *Electrochimica Acta*. 52(3).1033-1037. Nov 2006.

[28] Suffredini HB, Salazar-Banda GR, Avaca LA. Enhanced ethanol oxidation on PbOx-containing electrode materials for fuel cell applications. *Journal of Power Sources*. 171(2).355-362. Sep 2007.

[29] Huang MH, Wang F, Li LR, Guo YL. A novel binary Pt3Tex/C nanocatalyst for ethanol electro-oxidation. *Journal of Power Sources*. 178(1).48-52. Mar 2008.

[30] Lee KS, Park IS, Cho YH, et al. Electrocatalytic activity and stability of Pt supported on Sb-doped SnO2 nanoparticles for direct alcohol fuel cells. *Journal of Catalysis*. 258(1).143-152. Aug 2008.

[31] Bai YX, Wu JJ, Qiu XP, et al. Electrochemical characterization of Pt-CeO2/C and Pt-CexZr1-xO2/C catalysts for ethanol electro-oxidation. *Applied Catalysis B-Environmental*. 73(1-2).144-149. Apr 2007.

[32] Wang JS, Xi JY, Bai YX, et al. Structural designing of Pt-CeO2/CNTs for methanol electro-oxidation. *Journal of Power Sources*. 164(2).555-560. Feb 2007.

[33] Diaz DJ, Greenletch N, Solanki A, Karakoti A, Seal S. Novel nanoscale ceria-platinum composite electrodes for direct alcohol electro-oxidation. *Catalysis Letters*. 119(3-4).319-326. Dec 2007.

[34] Xu CW, Shen PK, Liu YL. Ethanol electrooxidation on Pt/C and Pd/C catalysts promoted with oxide. *Journal of Power Sources*. 164(2).527-531. Feb 2007.

[35] Bai YX, Wu JJ, Xi JY, et al. Electrochemical oxidation of ethanol on Pt-ZrO2/C catalyst. *Electrochemistry Communications*. 7(11).1087-1090. Nov 2005.

[36] Xu CW, Shen PK, Ji XH, Zeng R, Liu YL. Enhanced activity for ethanol electro oxidation on Pt-MgO/C catalysts. *Electrochemistry Communications*. 7(12).1305-1308. Dec 2005.

[37] Song HQ, Qiu XP, Li FS, Zhu WT, Chen LQ. Ethanol electro-oxidation on catalysts with TiO2 coated carbon nanotubes as support. *Electrochemistry Communications*. 9(6).1416-1421. Jun 2007.

[38] Lei B, Xue JJ, Jin DP, Ni SG, Sun HB. Fabrication, annealing, and electrocatalytic properties of platinum nanoparticles supported on self-organized TiO2 nanotubes. *Rare Metals*. 27(5).445-450. Oct 2008.

[39] Jiang QZ, Wu X, Shen M, Ma ZF, Zhu XY. Low-Pt content carbon-supported Pt-Ni-TiO2 nanotube electrocatalyst for direct methanol fuel cells. *Catalysis Letters*. 124(3-4).434-438. Aug 2008.

[40] Song HQ, Qiu XP, Li FH. Effect of heat treatment on the performance of TiO2-Pt/CNT catalysts for methanol electro-oxidation. *Electrochimica Acta*. 53(10).3708-3713. Apr 2008.

[41] Song HQ, Qiu XP, Guo DJ, Li FS. Role of structural H2O in TiO2 nanotubes in enhancing Pt/C direct ethanol fuel cell anode electro-catalysts. *Journal of Power Sources*. 178(1).97-102. Mar 2008.

[42] Liu B, Chen JH, Zhong XX, Cui KZ, Zhou HH, Kuang YF. Preparation and electrocatalytic properties of Pt-SiO2 nanocatalysts for ethanol electrooxidation. *Journal of Colloid and Interface Science*. 307(1).139-144. Mar 2007.

[43] Papaioannou E. I., Siokou A., Comninellis Ch., Katsaounis A., Pt–Ir Binary Electrodes for Direct Oxidation of Methanol in Low-Temperature Fuel Cells (DMFCs), *Electrocatalysis*, 4. 375–381. 2013.